Cell Reports
Medicine

Article

Adeno-associated-virus-mediated gene delivery to ovaries restores fertility in congenital infertile mice

Graphical abstract

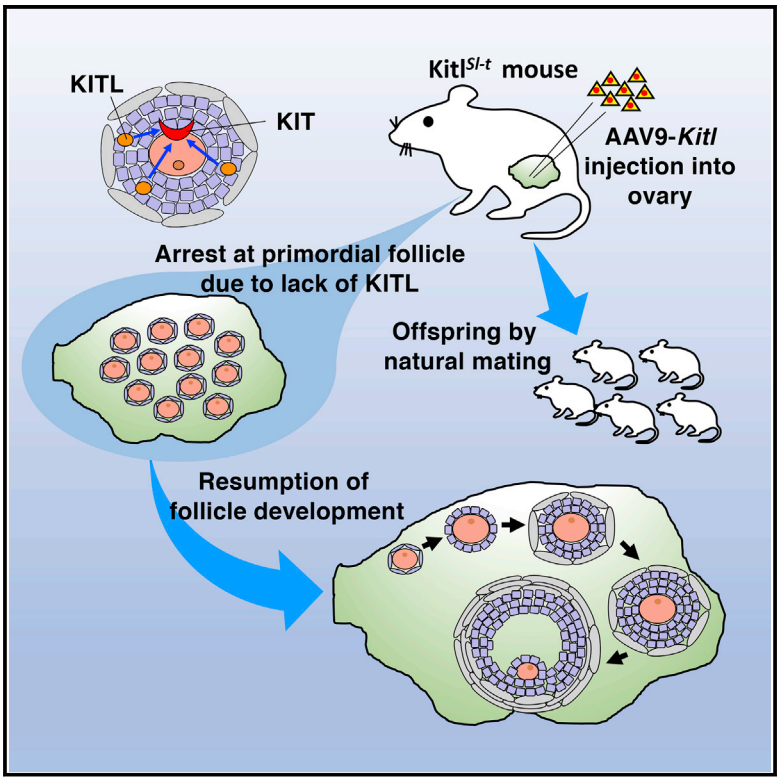

Authors

Mito Kanatsu-Shinohara, Jiyoung Lee, Takehiro Miyazaki, Hiroko Morimoto, Takashi Shinohara

Correspondence

tshinoha@virus.kyoto-u.ac.jp

In brief

Kanatsu-Shinohara et al. introduce a gene therapy for the treatment of congenital female infertility resulting from a granulosa defect. AAVs penetrate the blood-follicle barrier and infect granulosa cells without integration into the genome of the offspring. Results provide a basis of developing technologies for the treatment of human infertility.

Highlights

- AAVs can penetrate the blood-follicle barrier and infect granulosa cells
- AAVs rescue congenital infertility resulting from a granulosa defect
- No transgene integration is found in the genome of the offspring
- Offspring show normal genomic imprinting patterns

Kanatsu-Shinohara et al., 2022, Cell Reports Medicine *3*, 100606
May 17, 2022
https://doi.org/10.1016/j.xcrm.2022.100606

CellPress

Cell Reports Medicine

CellPress
OPEN ACCESS

Article

Adeno-associated-virus-mediated gene delivery to ovaries restores fertility in congenital infertile mice

Mito Kanatsu-Shinohara,[1,2] Jiyoung Lee,[3] Takehiro Miyazaki,[1] Hiroko Morimoto,[1] and Takashi Shinohara[1,2,4,*]
[1]Department of Molecular Genetics, Graduate School of Medicine, Kyoto University, Kyoto 606-8501, Japan
[2]AMED-CREST, Chiyoda-ku, Tokyo 100-0004, Japan
[3]Department of Epigenetics, Medical Research Institute, Tokyo Medical and Dental University (TMDU), Tokyo 113-8510, Japan
[4]Lead contact
*Correspondence: tshinoha@virus.kyoto-u.ac.jp
https://doi.org/10.1016/j.xcrm.2022.100606

SUMMARY

Oocytes and granulosa cells closely interact with each other during follicular development, and a lack of appropriate signaling between them results in infertility. Attempts to manipulate oocyte microenvironment have been impeded by the impermeability of the blood-follicle barrier (BFB). To establish a strategy for manipulating oogenesis, we use adeno-associated viruses (AAVs), which have a unique ability of transcytosis. Microinjecting of AAVs into the ovarian stroma penetrates the BFB and achieves long-term gene expression. Introduction of an AAV carrying the mouse *Kitl* gene restores oogenesis in congenitally infertile $Kitl^{Sl\text{-}t}/Kitl^{Sl\text{-}t}$ mutant mouse ovaries, which lack *Kitl* expression but contain only primordial follicles. Healthy offspring without AAV integration are born by natural mating. Therefore, AAV-mediated gene delivery not only provides a means for studying oocyte-granulosa interactions through the manipulation of the oocyte microenvironment but could also be a powerful method to treat female infertility resulting from somatic cell defects.

INTRODUCTION

The number of infertile couples is increasing, with almost 20% of the population unable to have children. Most cases of female infertility are associated with abnormal oocyte development or ovulation. Oogenesis is a complex process dependent on direct intraovarian interactions between germ cells and somatic cells as well as extraovarian factors that are coordinated by feedback control mediated by pituitary hormones.[1,2] After the mitotic division of oogonia, female germ cells enter meiosis and remain arrested at the prophase stage of the first meiotic division before birth. At the time of birth, all oocytes are surrounded by a single layer of follicular epithelial cells. These follicle cells develop into granulosa cells, which provide oocytes with the nutrients and regulatory signals necessary for promoting oocyte growth, nuclear maturation, and the acquisition of developmental competence. The granulosa cells secrete a basement membrane, which is then surrounded by thecal cells. During cyclic recruitment, only a limited number of growing follicles survive and develop to advanced stages, while the default pathway is to undergo atresia. Because of the close interaction between oocytes and granulosa cells, defects in granulosa cells can cause female infertility. Currently, there are no effective methods available to correct granulosa cell defects.

Several molecules are known to be involved in the crosstalk between oocytes and granulosa cells.[2] One of the primary molecules mediating this interaction is KITL. There are two isoforms of KITL: soluble (KITL1) and membrane-bound (KITL2) forms. The interaction between KITL and its receptor KIT, which are expressed by granulosa cells and oocytes, respectively, controls the initiation of follicular growth.[3] Because these genes are also involved in the survival of primordial germ cells, animals harboring KIT or KITL mutations have fewer germ cells and are generally infertile. KIT is involved in regulating several stages of oocyte development, including the onset of primordial follicle development, primary follicle growth, follicular fluid formation in preantral follicles, and penultimate-stage ovarian follicle maturation before ovulation.[3] Follicle-stimulating hormone (FSH) regulates KITL expression in a biphasic manner with low concentration of FSH increasing the relative abundance of KITL2, a membrane-bound isoform of KITL, which subsequently activates KIT receptors in oocytes.[4] In contrast, high FSH increases the KITL1/KITL2 ratio and fails to promote oocyte development, which underscores the physiological importance of membrane-bound KITL2 *in vivo*. Oocytes, in turn, regulate *Kitl* mRNA expression in granulosa cells in a stage-specific manner.[5] Therefore, *Kitl* is dispensable for primordial follicle formation but is necessary for subsequent oogenesis.

Given the close interaction between oocytes and granulosa cells, a valuable approach to better understanding of oogenesis would be to introduce genes into granulosa cells and then monitor the outcome. This technique could also be employed to correct defective granulosa cells. However, gene transduction into ovaries is dangerous because transgenes can potentially

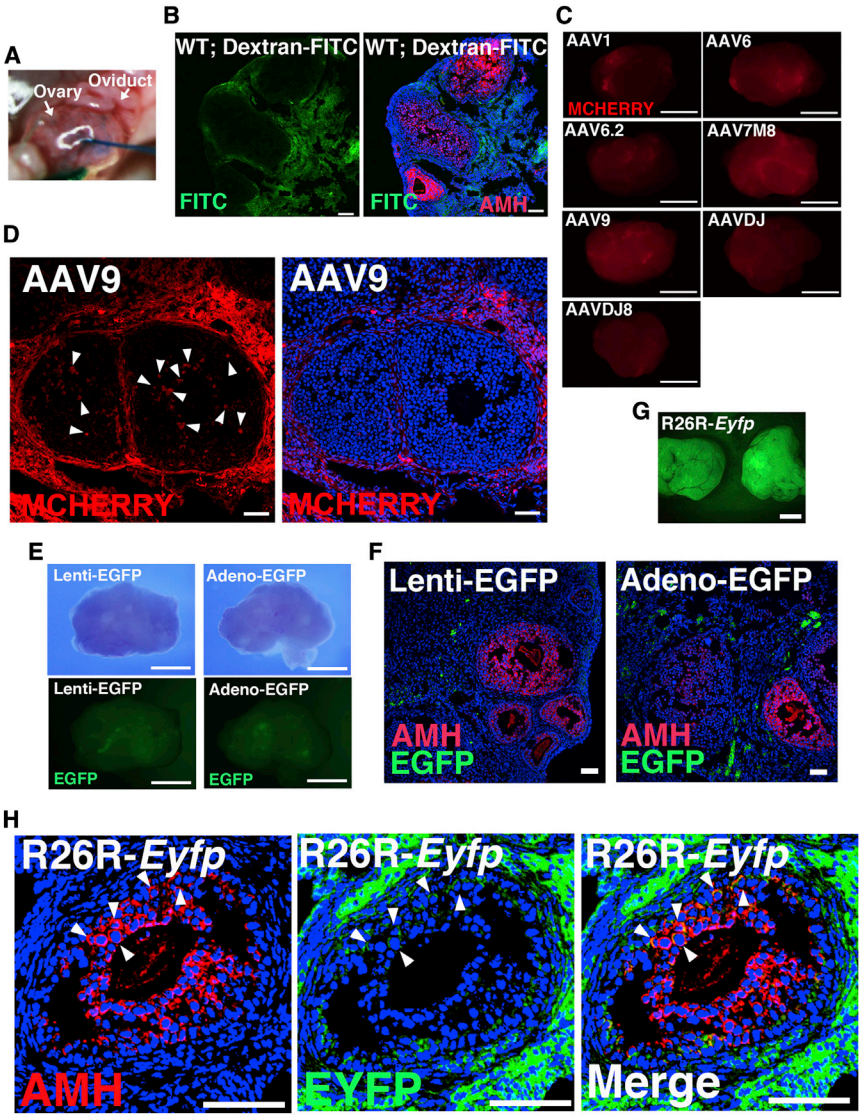

Figure 1. Screening of AAV serotypes

(A) Microinjection into the ovary.

(B) Functional assessment of the BFB. WT ovaries were injected interstitially with FITC-dextran (green). Samples were recovered 30 min after microinjection and immunostained with anti-AMH antibody to detect granulosa cells.

(C and D) Appearance (C) and histology (D) of ovaries 1 week after AAV-*mCherry* injection. Arrowheads indicate cells expressing MCHERRY.

(E and F) Appearance (E) and immunostaining (F) of ovaries after injection of lentivirus or adenovirus expressing EGFP.

(G and H) Appearance (G) and immunostaining (H) of *R26R-Eyfp* mouse ovaries 1 week after AAV9-*Cre* microinjection. Arrowheads indicate cells expressing AMH and EYFP.

Scale bars, 50 μm (B, D, F, and H) and 1 mm (C, E, and G). Counterstain, Hoechst 33342 (B, D, F, and H). See also Figures S1 and S2.

integrate into the genome of the oocytes. Because germline transgene integration is an important concern for gene therapy, several attempts have been reported to confirm the lack of germline integration after intravenous or intraperitoneal injection of virus vectors. However, no oocyte or granulosa cell infection has been reported.[6,7] Although adenovirus was used to treat infertility in one study,[8] the animals remained infertile. Although ovarian gene therapy has been attempted for cancer treatment,[9] no successful rescue of female infertility has been reported to date.

The purpose of this study was to establish a method for the introduction of genes into granulosa cells. Granulosa cells rest on a basal lamina that separates them from the vascularized theca interna, meaning that they have no direct blood supply. This "blood-follicle barrier (BFB)" serves as a molecular sieve, preventing the diffusion of proteins >20 nm in size.[10,11] We therefore hypothesized that penetrating the BFB would be key for successful gene transduction. Although adeno-associated viruses (AAVs) are too large (25 nm) to penetrate the BFB,[12] AAVs have a unique ability to undergo transcytosis;[13] we therefore pursued an AAV-based vector despite its size constraints and possibility of transducing oocytes because transcytosis can also promote transduction of oocytes. This method was applied successfully to treat congenitally infertile female mice. Our results not only reveal a remarkable flexibility of oocyte-granulosa cell interactions but also provide a possibility of gene therapy for female infertility in humans.

RESULTS

Screening of AAV serotypes by *in vivo* microinjection

To test the permeability of the BFB, we microinjected fluorescein isothiocyanate (FITC)-dextran (500 kDa) into wild-type (WT) ovaries. Using glass needles, virus particles were inserted under the tunica albuginea of ovaries and FITC-dextran was directly injected (Figures 1A and 1B). Although strong fluorescence signals were detected in the interstitium, no signals were found within the follicle, thus indicating the presence of the BFB. We then generated AAVs with various capsids (AAV1, AAV6, AAV6.2, AAV7M8, AAV9, AAVDJ, and AAVDJ8), all of which expressed *mCherry* under the ubiquitous CAG promoter. The viruses were then microinjected into the ovaries. Seven days after microinjection, the ovaries were analyzed under UV light. All injected ovaries showed fluorescent signals but to varying degrees (Figures 1C and S1A). To compare the effectiveness of transducing granulosa cells, we carried out immunostaining. Theca cells, which express HSD3B, displayed relatively strong signals compared with granulosa cells. Although most of the tested

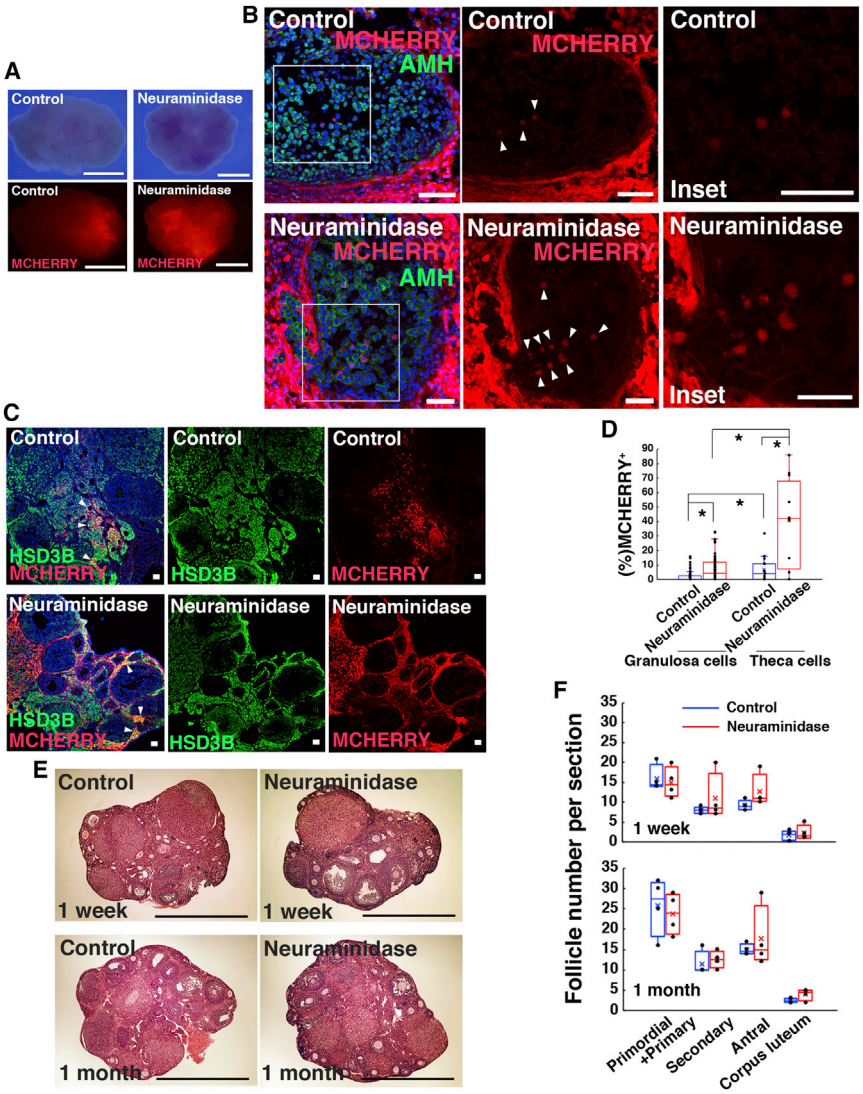

Figure 2. Improvement of AAV9 transduction by neuraminidase

(A) Appearance of WT ovaries 1 week after co-injection with AAV9-*mCherry* and neuraminidase.

(B) Immunostaining of granulosa cells with anti-AMH antibody. Arrowheads indicate cells expressing MCHERRY.

(C) Immunostaining of theca cells with anti-HSD3B antibody. Arrowheads indicate cells expressing MCHERRY.

(D) Quantification of immunostaining (n = 43–56 cells for AMH; n = 12–15 cells for HSD3B). Statistics with t test are shown.

(E) Histology of ovaries 1 week and 1 month after virus injection.

(F) Quantification of developing oocytes after neuraminidase injection (n = 4 ovaries). Statistics with t test are shown.

Scale bars, 1 mm (A and E) and 50 μm (B and C). Counterstain, Hoechst 33342 (B and C) and H&E (E). *p < 0.05. Data are represented as mean ± SEM. See also Figure S3.

AAVs rarely infected AMH$^+$ granulosa cells, AAV9 showed the strongest signal in granulosa cells (Figures 1D and S1B–S1D). Despite the infection of granulosa cells, no signal was present in the oocytes. These results suggested that AAV9 penetrated the BFB and infected granulosa cells without transducing oocytes. Therefore, we selected AAV9 for further experiments.

The microinjection of AAV9 did not appear to affect ovarian follicle development, because normal-looking follicles were present throughout the ovary. To determine whether the BFB penetration was specific to AAVs, we microinjected adenovirus or lentivirus that expresses EGFP (Figure 1E). Following this, no EGFP signals were detected in the follicles (Figure 1F).

To confirm that AAV9 was not able to infect oocytes, we next used *R26R-Eyfp* mice, as they enabled the more sensitive detection of infected cells.[14] *R26R-Eyfp* mice contain a *loxP*-flanked STOP sequence followed by the *Eyfp* gene, which is inserted into the Gt(ROSA)26Sor locus. We generated a *Cre*-expressing AAV9 variant and monitored the expression of EYFP. EYFP signal was detected in ovaries collected at as early as 2 days after microinjection, and its expression in AMH$^+$ granulosa cells did not change significantly even at 1 month after microinjection (Figures 1G, S2A, and S2B). EYFP$^+$ infected cells were distributed throughout the ovary, despite injecting into the superficial area of the ovarian stroma. However, no signals were detected within the oocytes (Figure 1H). These results suggested that AAV9 did not infect oocytes.

Improvement of transduction of AAV9 by neuraminidase

Although our results so far indicated successful transduction of granulosa cells, the efficiency was still limited. To improve the infection efficiency, we injected neuraminidase alongside AAV9. AAV9 uptake in lungs was greatly increased when the terminal sialic acids of the virus target cells were removed by neuraminidase.[15] In the current experiment, we co-injected AAV9-*mCherry* with neuraminidase and analyzed the expression by real-time PCR. Examination at 1 week after injection showed a significant increase of *mCherry* mRNA by neuraminidase supplementation (Figure S3A), although this increase in MCHERRY expression was not confirmed by western blotting (Figure S3B). Nevertheless, the ovaries that had received co-injection of neuraminidase appeared to express MCHERRY more strongly (Figure 2A). Immunostaining showed that neuraminidase co-injection increased the area of MCHERRY expression in both AMH$^+$ granulosa cells and HSD3B$^+$ theca cells (Figures 2B–2D). The higher efficiency of theca cell transduction suggests that they have a different carbohydrate synthesis mechanism and express more exposed galactose residues, which is considered to bind AAV9.[15] It is also possible that theca cells were

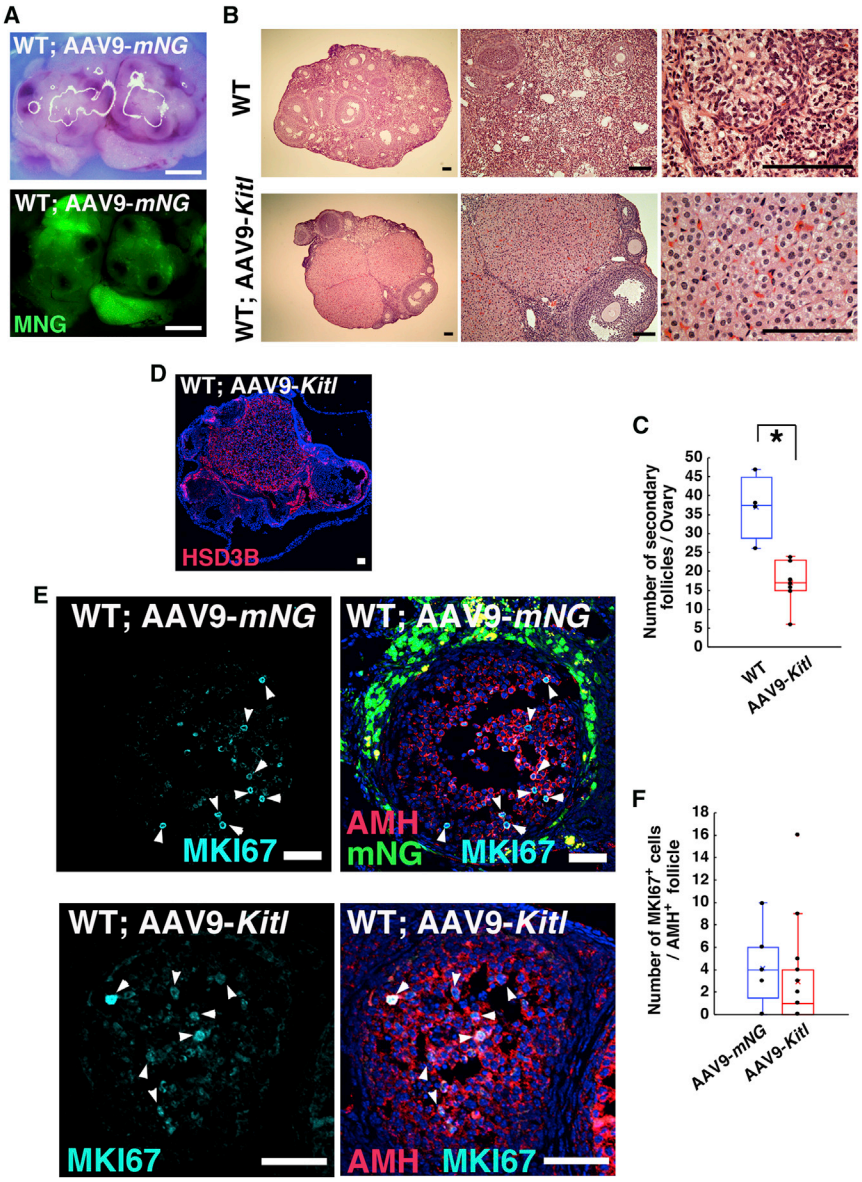

Figure 3. Functional analysis of AAV9-*Kitl* transduction in WT mice

(A) Appearance of ovary after AAV9-*mNG* injection.
(B) Histology of ovaries after AAV9-*Kitl* injection.
(C) Quantification of secondary follicles (n = 4–7 ovaries). Statistics with t test are shown.
(D) Immunostaining with anti-HSD3B antibody.
(E) Double immunostaining with anti-AMH and MKI67 antibodies. Arrows indicate cells expressing MKI67.
(F) Quantification of cells (n = 9–15 follicles) with signals. Statistics with t test are shown.
Scale bars, 1 mm (A), 100 μm (B), and 50 μm (D and E). Counterstain, H&E (B) and Hoechst 33342 (D and E). *$p < 0.05$. Data are represented as mean ± SEM. See also Figures S3, S4, and S5.

exposed to higher concentrations of neuraminidase and exposed galactose residues more efficiently due to limited diffusion after injection. Despite the increase in efficiency, we did not detect any signal in oocytes, and normal growing oocytes were found after co-injection of AACV9 and neuraminidase (Figure 2E). The number of follicles at different stages of development did not change significantly at 1 week and 1 month after virus injection (Figure 2F). These results showed that neuraminidase co-injection could improve AAV9 transduction efficiency without apparently interfering oogenesis.

Impact of AAV transduction on reproductive performance

Our results suggested that AAV9 can penetrate the BFB and reach the oocyte-granulosa complex without transducing the oocytes; we therefore attempted to manipulate the oocyte microenvironment by expressing *Kitl* and examined its impact on oogenesis and fertility. We microinjected *Kitl*-expressing AAV9 into 10 WT female mice; we speculated that the overexpression of *Kitl* might activate too many oocytes and lead to sterility. As a control, we microinjected AAV9-expressing *mNeonGreen* (*mNG*) (Figure 3A); the same concentration of AAV9-*Kitl* was microinjected into the ovaries of nine mice of the same age. Real-time PCR analysis showed increased expression of *Kitl* following AAV9-*Kitl* injection. *Kitl* expression was significantly enhanced by neuraminidase supplementation (Figure S3C). However, the increase in KITL expression was not confirmed by western blotting (Figure S3D). Nevertheless, because timing of protein expression analysis might not have been appropriate, AAV-injected females were mated with a WT male mouse 1 week after AAV injection, and we recorded the number of offspring for 3 months.

In total, 8 of 10 mice were fertile after injection with AAV9-*Kitl*, while all nine control mice produced offspring. Sixteen litters were born from eight females transduced with AAV9-*Kitl* during the 3 months, whereas a total of 20 litters were born from nine females transduced with AAV9-*mNG* during the same period. For AAV9-*Kitl*, the litter size ranged from 1 to 12 with an average of 5.4. Likewise, the litter size ranged from 2 to 11 with an average of 5.6 for AAV9-*mNG*. In terms of the speed of offspring production, one of the eight females with AAV9-*Kitl* produced offspring as early as 28 days after microinjection. On the other hand, the first offspring from nine AAV9-*mNG* were born after 32 days. The average time taken for the first litter was 38.4 and 41.3 days for AAV9-*Kitl* and AAV9-*mNG* recipients, respectively. However, this difference was not significant. The oocyte pool was not exhausted in AAV9-*Kitl* transduced mice, as 6 of 8 (75.0%) females

CellPress
OPEN ACCESS

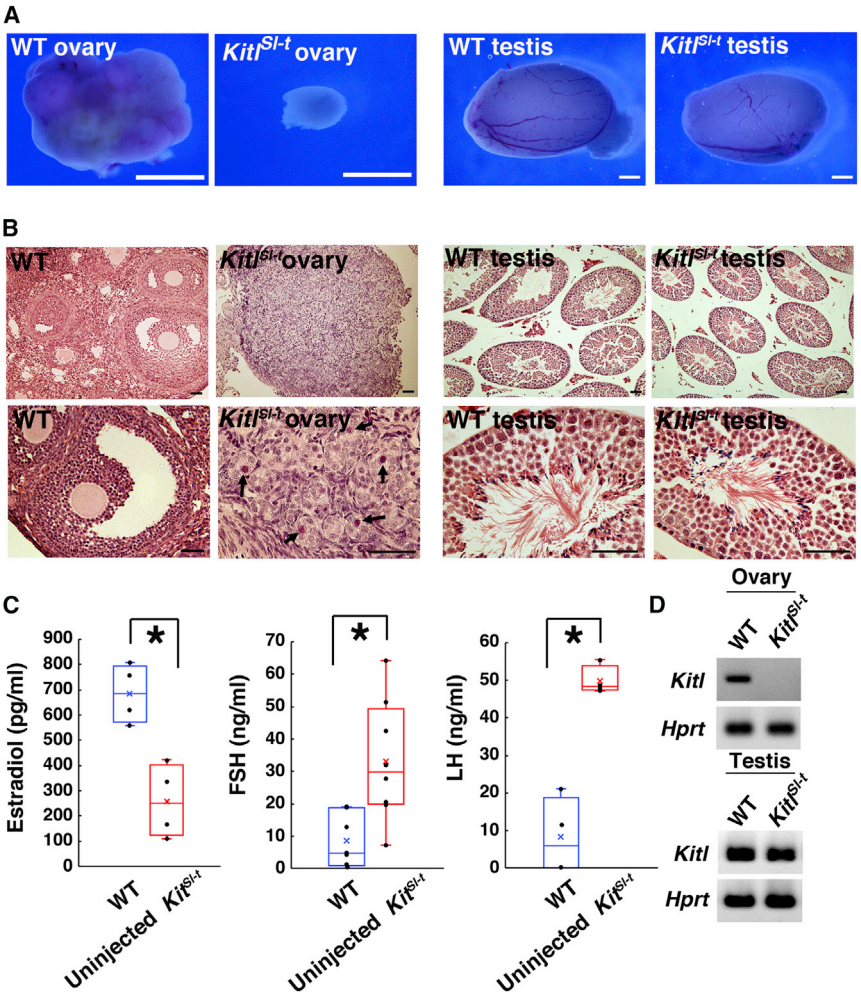

Figure 4. Analysis of $Kitl^{Sl\text{-}t}/Kitl^{Sl\text{-}t}$ mutant mice

(A and B) Appearance (A) and histology (B) of $Kitl^{Sl\text{-}t}/Kitl^{Sl\text{-}t}$ gonads. Arrows indicate oocytes.

(C) Hormone levels in peripheral blood (n = 4 animals). Statistics with t test are shown.

(D) RT-PCR analysis of *Kitl* expression.

Scale bars, 1 mm (A) and 50 μm (B). *p < 0.05. Data are represented as mean ± SEM. See also Figure S6.

Restoration of fertility in congenitally infertile mouse model by AAV transduction

We next attempted to rescue mice defective in oogenesis due to a *Kitl* mutation ($Kitl^{Sl\text{-}t}$).[16] Male $Kitl^{Sl\text{-}t}/Kitl^{Sl\text{-}t}$ mice are fertile, and the size of their testes are comparable to those of WT mice, whereas the ovaries of female $Kitl^{Sl\text{-}t}/Kitl^{Sl\text{-}t}$ mice are comparatively very small (Figure 4A). Histological analyses of $Kitl^{Sl\text{-}t}/Kitl^{Sl\text{-}t}$ mice showed that all follicles were arrested at an early stage with one layer of granulosa cells (Figure 4B). Consistent with this observation, 0 of >100 females produced offspring when caged with male mice. Peripheral blood samples taken from $Kitl^{Sl\text{-}t}/Kitl^{Sl\text{-}t}$ mice exhibited lower estrogen levels compared with the WT, while FSH and luteinizing hormone (LH) levels were significantly higher (Figure 4C); this resembles premature ovarian insufficiency in humans. A comparison of the WT *Kitl* and $Kitl^{Sl\text{-}t}$ sequences indicated two point mutations (Figure S6). Although the point mutation at position 42 (T→C) in the *Kitl* sequence in $Kitl^{Sl\text{-}t}/Kitl^{Sl\text{-}t}$ mice was silent, the second mutation at position 619 (G→T) resulted in an amino acid change from alanine to serine at amino acid position 207. However, this mutation is probably not responsible for the ovarian defect because male mutants exhibited normal spermatogenesis, which is also dependent on *Kitl* (Figure 4B). Following RT-PCR analysis, *Kitl* mRNA expression was undetectable in $Kitl^{Sl\text{-}t}/Kitl^{Sl\text{-}t}$ female mice (Figure 4D). It is therefore likely that the mutation responsible for the $Kitl^{Sl\text{-}t}$ phenotype disrupts a regulatory mechanism, which reduces levels of *Kitl* mRNA in the ovary.

We next examined whether oogenesis can be restored in $Kitl^{Sl\text{-}t}/Kitl^{Sl\text{-}t}$ mice by transducing ovaries with an AAV expressing functional *Kitl*. We microinjected AAV9-*Kitl* (1.5×10^{12}/mL to 7.0×10^{14}/mL) into the ovaries of adult female $Kitl^{Sl\text{-}t}/Kitl^{Sl\text{-}t}$ mice. Neuraminidase was co-injected in some experiments to improve the transduction efficiency. Real-time PCR showed that microinjection of AAV9-*Kitl* restored *Kitl* expression in mutant ovaries, although *Kitl* expression was still weaker compared with that in WT ovaries (Figure S3E). After virus injection, we collected mutant ovaries at different time points could produce two litters within 3 months. Seven of nine (77.8%) females produced two litters after AAV9-*mNG* transduction.

We made histological sections of the ovaries to examine the impact of *Kitl* overexpression after AAV9 transfection. Although normal oogenesis was evident after *Kitl* overexpression, we noted a significant expansion of $HSD3B^+$ theca cells in several areas (Figure 3B), which suggested that unphysiological hyperactivation of KIT occurred in theca cells because they also express KIT.[3] Moreover, we also observed significant decrease in the number of secondary follicles (Figure 3C). Immunostaining confirmed the increase in $HSD3B^+$ theca cells (Figure 3D) but did not show apparent difference in the number of $MKI67^+$ granulosa cells between AAV9-*Kitl*- and AAV9-*mNG*-injected ovaries (Figures 3E and 3F). Despite the significant increase in theca cell number, *Kitl* overexpression did not induce oocyte apoptosis (Figure S4A). Although AAVs can cause inflammation, no apparent infiltration of $CD4^+$ or $CD8^+$ cells was detected (Figures S4B and S4C). PCR analysis of the offspring showed that the transgenes had not been integrated (Figure S5). These results showed that AAV9-*Kitl* overexpression allowed complete oogenesis without the risk of transgene integration into the genome of oocytes.

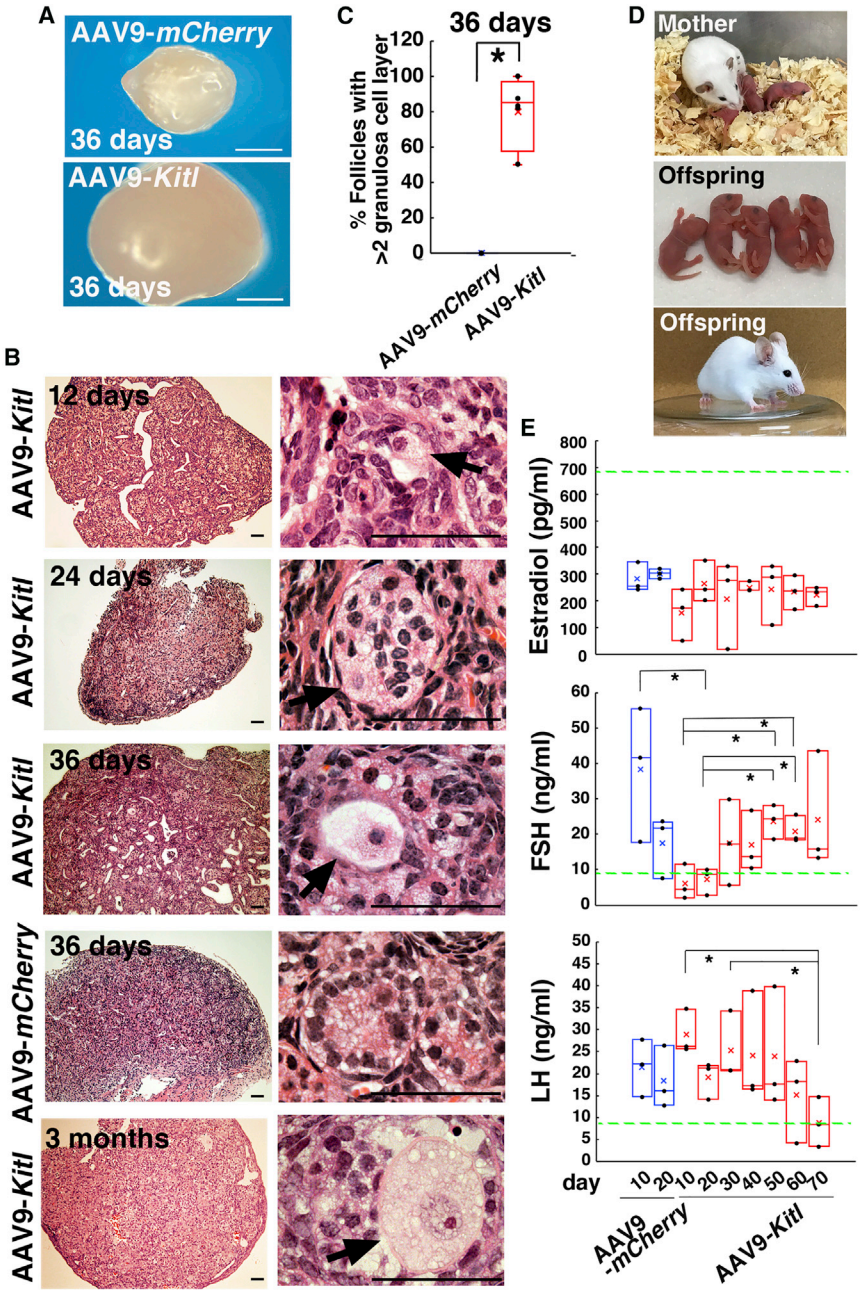

Figure 5. Rescue of infertility in *Kitl*$^{Sl\text{-}t}$/*Kitl*$^{Sl\text{-}t}$ mutant mice by AAV9-*Kitl* infection

(A and B) Appearance (A) and histology (B) of *Kitl*$^{Sl\text{-}t}$/*Kitl*$^{Sl\text{-}t}$ ovary after AAV9-*Kitl* injection. Arrows indicate growing oocytes.

(C) Quantification of follicles with two layers of granulosa cells (n = 8 ovaries). Statistics with t test are shown.

(D) Offspring born after AAV9-*Kitl* injection.

(E) Hormone levels in peripheral blood in *Kitl*$^{Sl\text{-}t}$/*Kitl*$^{Sl\text{-}t}$ mutant mice after AAV9-*Kitl* infection (n = 3 animals). Samples were analyzed after mating experiments. Green lines indicate control hormone levels in WT mice (average values from Figure 4C). Statistics with t test are shown.

Scale bars, 500 μm (A) and 50 μm (B). Counterstain, H&E (B). *$p < 0.05$. Data are represented as mean ± SEM. See also Figure S3.

and analyzed the impact of virus transduction. While the non-injected ovaries were small, those that received AAV-*Kitl* injections were significantly larger (Figure 5A). Histological analyses revealed that the ovaries of *Kitl*$^{Sl\text{-}t}$/*Kitl*$^{Sl\text{-}t}$ mice that had received the AAV-*Kitl* injection contained developing follicles (Figure 5B). Although the frequency of growing follicle was very low (<1 oocyte per section), the follicles were larger and several had more than two layers of granulosa cells (Figure 5C), suggesting that AAV9-*Kitl* injection caused oogenesis to resume and induced granulosa cell proliferation. Constitutive KIT signaling can cause tumorigenesis,[17] and we found increased theca cells in WT ovaries (Figure 3B); however, no evidence of tumor formation or expansion of theca cell population was found. In contrast, no growing oocytes were found by injection of AAV9-*mCherry* (Figure 5C). These results suggested that oocyte-granulosa interactions that resembled the WT had occurred in ovarian follicles following AAV9-*Kitl* microinjection.

We then mated the rest of the AAV-*Kitl*-injected *Kitl*$^{Sl\text{-}t}$/*Kitl*$^{Sl\text{-}t}$ females with homozygous *Kitl*$^{Sl\text{-}t}$/*Kitl*$^{Sl\text{-}t}$ males to test whether AAV-*Kitl* can restore fertility. Overall, 8 of 19 (42.1%) females became fertile in five experiments (Table 1). Offspring with normal sex ratios were born as early as 62 days after microinjection (Figure 5D). It took an average of 65.6 days after viral microinjection to obtain the first litter, but no offspring were born after 126 days. The average number of offspring was 3.1 ± 0.7 per litter (n = 9). The offspring were morphologically normal at birth. Although there may have been too few mice to detect a significant effect of neuraminidase co-injection on fertility, increasing the viral concentration appears to increase the fertility rate (Table 1). When the offspring became sexually mature, the females were infertile due to the *Kit*$^{Sl\text{-}t}$ mutations inherited from their homozygous *Kitl*$^{Sl\text{-}t}$/*Kitl*$^{Sl\text{-}t}$ parents, while the male offspring were fertile. All mature offspring had a white coat color (Figure 5D), which was due to a lack of melanocytes in this strain. Although most of the females only produced one litter, one of the fertile females produced two litters (Table 1).

Because these results indicated a normal oocyte cycle, we analyzed hormonal levels in the peripheral blood of three mice that received AAV-*Kitl* microinjection. As expected, we found dynamic changes in FSH and LH levels in AAV9-*Kitl*-transduced

Table 1. Progeny from *Kitl*$^{Sl\text{-}t}$/*Kitl*$^{Sl\text{-}t}$ mice injected with *Kitl*-expressing AAVs

Exp	No. of animals	Fertile animals (%)	Virus titer	Neuraminidase	Days to progeny	Number of offspring
No. 1	2	1 (50)	1.5×10^{12}	–	59[a]	4
No. 2	5	1 (20)	3.9×10^{13}	–	62[b]	7
No. 3	3	1 (33.3)	2.9×10^{14}	+	72	2
No. 4	2	0	2.9×10^{13}	+	NA	0
No. 5	7	5 (71.4)	7.0×10^{14}	+	63	16

All females were mated with *Kitl*$^{Sl\text{-}t}$/*Kitl*$^{Sl\text{-}t}$ male to confirm the genotype of the offspring. NA, not applicable.
[a]Pregnant mother was sacrificed.
[b]The same female sired another offspring (126 days after microinjection).

animals when compared with untreated *Kitl*$^{Sl\text{-}t}$/*Kitl*$^{Sl\text{-}t}$ mice (Figure 5E). FSH levels decreased significantly within 10 days after AAV injection. On the other hand, we were not able to find significant changes in LH levels until 70 days after virus injection. We did not observe significant changes in estrogen levels.

We carried out a series of experiments using a lentivirus that expresses *Kitl*. However, none of the 12 females that received the virus produced offspring. Because lentivirus vectors did not penetrate the BFB (Figure 1F), these results suggested that infection of granulosa cells is critical for restoration of fertility in *Kitl*$^{Sl\text{-}t}$/*Kitl*$^{Sl\text{-}t}$ mice. To confirm the specificity of the serotype, we used another vector (AAV7M8-*Kitl*);[18] however, none of the eight animals became fertile. Because AAV9 showed more extensive infection of granulosa cells, these results suggested that AAV serotype was critical for the restoration of fertility.

DNA analysis of the offspring

To determine whether the offspring of the AAV-*Kitl*-injected *Kitl*$^{Sl\text{-}t}$/*Kitl*$^{Sl\text{-}t}$ mice had integrated the AAV into their genome, we selected one of the litters and examined their genomic DNA by Southern blotting (Figure 6A). Following hybridization with an AAV-specific probe, no genomic integration of the AAV vector was apparent. We then performed PCR using AAV-specific primers; none of the offspring contained AAV DNA (Figure 6B). Using this protocol, we analyzed all offspring by PCR using AAV-specific primers and found no evidence of germline integration of the transgene integration.

Genome imprinting in the female germline occurs postnatally.[19] Therefore, it was possible that *Kitl* overexpression might have caused abnormal DNA imprinting. To test this possibility, we carried out combined bisulfite restriction analysis (COBRA) on the DNA of mature offspring. The differentially methylated regions (DMRs) of *H19* and *Igf2r* revealed the somatic cell DNA methylation patterns (Figure 6C). We further analyzed the DNA of two offspring (one male and one female) by bisulfite DNA sequencing, which confirmed that the DNA methylation patterns of both offspring were normal (Figure 6D). These results demonstrated that ovaries injected with AAV-*Kitl* were able to produce fertile oocytes, which could develop into normal offspring.

DISCUSSION

The importance of the molecular interactions between oocytes and granulosa cells is well recognized; however, methods to understand their interactions are currently limited. This hampers our understanding of oogenesis, as well as the development of techniques for treating female infertility. In this study, we demonstrated that AAVs can be used to transduce ovarian follicles *in vivo*. Furthermore, the introduction of WT *Kitl* cDNA into the granulosa cells restored fertility in congenitally infertile *Kitl*$^{Sl\text{-}t}$/*Kitl*$^{Sl\text{-}t}$ mice. Because no transgene was found in the offspring, these results raise a possibility of conducting AAV-based gene therapy for the treatment of female infertility.

An important observation from this study was the penetration of the BFB by AAV9. AAVs are considered to be the most promising viral vectors for gene therapy.[20] Although we currently do not know how AAVs could penetrate the BFB, it is likely that they passed the BFB via transcytosis.[13] Transcytosis is a type of transcellular transport in which various macromolecules are transported across the interior of a cell. *In vitro* experiments showed that AAV5 penetrated reconstituted endothelial cells and epithelia, which were blocked by AAV5-specific antisera or tannic acid.[13] Although transcytosis has not been reported for any cell type in the ovary, we speculate that AAV9 migration through the BFB is regulated by a similar process. However, if this is the case, it is also possible that AAVs might have transduced oocytes via transcytosis, although we did not find evidence of infection in DNA analysis of the offspring. We found little signals using lentivirus or adenovirus. In particular, relatively poor theca cell transduction by lentivirus suggests that vesicular stomatitis virus G protein (VSV-G) is not suited for transducing these cells. However, there is still room for improvement. For example, modification of the virus envelope might improve infection levels and patterns, as we previously demonstrated for testis.[21] Further investigation will be required to address these points.

The most striking result from the present study was the production of offspring from *Kitl*$^{Sl\text{-}t}$/*Kitl*$^{Sl\text{-}t}$ mice, which occurred despite the complete lack of endogenous *Kitl* expression in the ovary. Our results demonstrated that *Kitl*$^{Sl\text{-}t}$/*Kitl*$^{Sl\text{-}t}$ oocytes, which had never been able to differentiate beyond meiotic arrest during development to sexual maturity, could reinitiate oogenesis and develop into functional oocytes. The restoration of oogenesis in adult mutants suggests a remarkable flexibility in granuloma-oocyte interactions. Fertility restoration by natural mating was unexpected, because sperm and embryos are actively transported in the oviduct via the pacemaker activity of interstitial cells of Cajal, which form a dense network associated with smooth muscle cells. The KITL-KIT interaction is important for development of Cajal cells.[22] Because lack of melanocyte in this strain suggested defective neural crest development, we did not expect the mutant

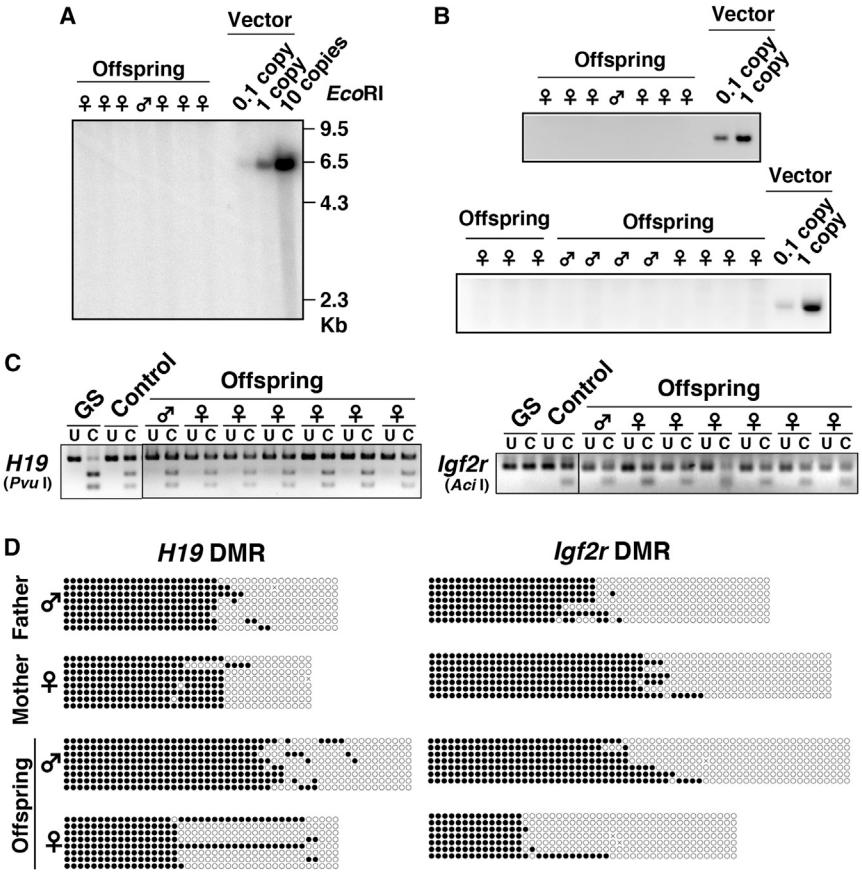

Figure 6. DNA analysis of the offspring

(A and B) Southern blot (A) and PCR (B) analyses of F1 DNA samples from *Kitl*$^{Sl\text{-}t}$/*Kitl*$^{Sl\text{-}t}$ mutant mice. Controls represent viral DNA in amounts equivalent to indicated copies of viral DNA per diploid genome. DNA was digested with the indicated restriction enzymes (A). Control DNA data were derived from the same blotting experiment.

(C) DMR methylation of *H19* and *Igf2r* by COBRA. DNA from germline stem (GS) cells was used as a positive control.

(D) DMR methylation of *H19* and *Igf2r* by bisulfite sequencing. Black ovals indicate methylated cytosine-guanine sites (CpGs), and white ovals indicate unmethylated CpGs.

oocyte to be fertilized and subsequently transported via oviduct for implantation in uterus with abnormal hormone patterns.

At least two questions arise from our results. The first is regarding the mechanism of hormonal regulation. While FSH levels dropped significantly soon after virus injection, we did not find apparent changes in estrogen levels. Moreover, it took more than 60 days for LH levels to decrease significantly. We speculate that such abnormalities may be caused, in part, by the loss of AAV-infected follicle cells. Because AAVs do not integrate into the host genome, they would be gradually lost in dividing cells. Because granulosa cells increase their number during oogenesis, it is likely that the mutant ovaries eventually lost KITL-expressing granulosa cells. Alternatively or in addition, the hypothalamic-pituitary-ovarian axis may still be immature soon after AAV transduction. The second question is regarding how the number of oocytes released at ovulation is regulated. KITL was likely expressed throughout the ovaries; we hypothesized that this constitutive KITL expression could have recruited a large number of oocytes for ovulation. However, AAV transduction did not significantly impact litter size, as AAV-*Kitl*-transduced mice produced litters that were within the normal range of WT mice. Elucidating the mechanisms of these phenomena will provide valuable insight on the dynamics and flexibility of the female reproductive system.

Vector integration into the germline is a crucial concern. Although AAVs rarely integrate into the host genome, several studies in somatic cells clearly showed integration into the host genome.[23,24] Therefore, evaluating the risk of germline integration would be a prerequisite for clinical application. So far, the likelihood of germline integration has only been investigated in subjects that have been intravenously or intraperitoneally injected. In the present study, the lack of transgene DNA in the offspring following direct ovarian injection suggests that AAV injection may be safe. We did not detect any fluorescent signals in oocytes after transducing R26R-*Eyfp* mice; therefore, it is unlikely that the oocytes were infected by the AAV. However, it is still possible that short-term virus exposure was insufficient for transducing oocytes. Moreover, our detection methods might not have been sensitive enough to find oocyte infection *in situ*. High-throughput DNA sequencing analysis of both parental oocyte-granulosa complex and the progeny will probably increase the sensitivity of virus integration in future studies. It would also be necessary to determine the infectivity of AAV9 in other animal models, because AAVs of the same serotype often have different targets depending on the animal species.[20] Additional screening of AAV serotypes and their receptor expression will be necessary to confirm the safety and serotypes that can be used for human infertility treatment.

Despite the success of this work, efforts to increase the transduction efficiency and fertility are still needed. More than half of the injected mice remained infertile, and only one of the fertile mice could produce two litters. Because we currently do not know why the mutant mice could not continue to generate offspring, we cannot totally exclude the possibility that AAV transduction may have a negative impact on reproductive performance. It is necessary to perform long-term fertility tests to confirm the effectiveness and side effects of the current approach. There are at least two possible approaches to improve the technique; one is the screening of capsids. Thecal cells were infected by AAV9, which caused an increase in their number.

Although we did not find significant impact in mutant ovaries, it is possible that infection of extrafollicular cells might have limited reproductive performance. Identification of more specific capsids with higher transduction efficiency may solve this problem. Another solution is to employ *in vitro* oocyte culture. Although the number of ovulated oocytes is small *in vivo*, numerous preovulatory follicles can be stimulated for simultaneous maturation *in vitro*. Because *in vitro* ovary culture can promote oocyte maturation to offspring production,[25] it would increase the efficiency of offspring production. Moreover, infection can be performed in a controlled manner with higher concentration of AAVs.

Our results, although in mice, suggest that some cases of female infertility in humans may be treated by AAV-mediated gene therapy. There is currently no effective method to treat premature ovarian insufficiency, which affects 1% of women by 40 years of age.[26] Adoption or oocyte donation is commonly recommended for patients who have not completed child bearing at the time of diagnosis. However, our successful rescue of congenitally infertile female mice creates a new possibility for infertile women, even after sexual maturation. The extensive generation and study of mouse mutants and molecular analysis of human patients have revealed a number of candidate genes that are potentially involved in ovarian failure,[27] including FSHR, FOXL2, and INHA. Investigating the timing and expression patterns of these candidate genes will help to determine the feasibility of gene therapy for female infertility. Thus, our study provides a new experimental strategy to genetically manipulate the oocyte microenvironment, which may be applied to cure human infertility, albeit with extreme caution.

Limitations of the study

Although we were able to demonstrate the expression of *Kitl* mRNA in AAV-*Kitl*-injected $Kitl^{Sl\text{-}t}/Kitl^{Sl\text{-}t}$ mice by real-time PCR, we were not able to demonstrate its protein expression. Because their ovaries are too small, even after AAV injection, it was not possible to collect sufficient amount of protein for such analysis. Moreover, we also failed to determine the best timing of analysis for AAV expression due to limitation in the number of mutant mice. The number of mutant granulosa cells probably changes dynamically after AAV transduction, which makes it difficult to find optimal time points for maximum protein expression. Future research using larger sample sizes is needed to address these issues.

For fertility experiments using WT mice, no overt abnormalities were observed at least within the 3-month mating period. Whether or not the AAV9 transfection has any potential effect on the reproductive life span of the treated females warrants further analysis.

STAR★METHODS

Detailed methods are provided in the online version of this paper and include the following:

SUPPLEMENTAL INFORMATION

Supplemental information can be found online at https://doi.org/10.1016/j.xcrm.2022.100606.

ACKNOWLEDGMENTS

Financial support for this research was provided by The Uehara Memorial Foundation, Takeda Science Foundation, AMED (17933225 and JP21gm1110008), and MEXT (19K22512, 19H05750, 19H04906, 18H04882, 18H05281, and 18H02935).

AUTHOR CONTRIBUTIONS

M.K.-S. and T.S. conceived the experiments. M.K.-S., J.L., T.M., H.M., and T.S. performed the experiments. M.K.-S. and T.S. wrote the paper.

DECLARATION OF INTERESTS

The authors declare no competing interests.

Received: October 20, 2021
Revised: January 24, 2022
Accepted: March 24, 2022
Published: April 27, 2022

REFERENCES

1. Gosden, R.G. (2013). Oocyte development and loss. Semin. Reprod. Med. *31*, 393–398.
2. Matzuk, M.M., Burns, K.H., Viveiros, M.M., and Eppig, J.J. (2002). Intracellular communication in the mammalian ovary: oocytes carry the conversation. Science *296*, 2178–2180.
3. Yoshida, H., Takakura, N., Kataoka, H., Kunisada, T., Okamura, H., and Nishikawa, S.-I. (1997). Stepwise requirement of c-kit tyrosine kinase in mouse ovarian follicle development. Dev. Biol. *184*, 122–137.
4. Kidder, G.M., and Vanderhyden, B.C. (2010). Bidirectional communication between oocytes and follicle cells: ensuring oocyte developmental competence. Can. J. Physiol. Pharmacol. *88*, 399–413.
5. Joyce, I.M., Pendola, F.L., Wigglesworth, K., and Eppig, J.J. (1999). Oocyte regulation of Kit ligand expression in mouse ovarian follicles. Dev. Biol. *214*, 342–353.
6. Pañeda, A., Vanrell, L., Mauleon, I., Crettaz, J.S., Berraondo, P., Timmermans, E.J., Beattie, S.G., Twisk, J., van Deventer, S., Prieto, J., et al. (2009). Effect of adeno-associated virus serotype and genomic structure on liver transduction and biodistribution in mice of both genders. Hum. Gene Ther. *20*, 908–917.
7. Kano, M., Sosulski, A.E., Zhang, L., Saatcioglu, H.D., Wang, D., Nagykery, N., Sabatini, M.E., Gao, G., Donahoe, P.K., and Pépin, D. (2017). AMH/MIS

as a contraceptive that protects the ovarian reserve during chemotherapy. Proc. Natl. Acad. Sci. U S A. *114*, E1688–E1697.

8. Ghadami, M., El-Demerdash, E., Salama, S.A., Binhazim, A.A., Archibong, A.E., Chen, X., Ballard, B.R., Sairam, M.R., and Al-Hendy, A. (2010). Toward gene therapy of premature ovarian failure: intraovarian injection of adenovirus expressing human FSH receptor restores folliculogenesis in FSHR(-/-) FORRKO mice. Mol. Hum. Reprod. *16*, 241–250.
9. Áyen, Á., Martinez, Y.J., Marchal, J.A., and Boulaiz, H. (2018). Recent progress in gene therapy for ovarian cancer. Int. J. Mol. Sci. *19*, 1930.
10. Gosden, R.G., Hunster, R.H.F., Telfer, E., Torrance, C., and Brown, N. (1988). Physiological factors underlying the formation of ovarian follicular fluid. J. Reprod. Fertil. *82*, 813–825.
11. Zachariae, F. (1958). Studies on the mechanism of ovulation: permeability of the blood-liquor barrier. Acta Endocrinologica *27*, 339–342.
12. Horowitz, E.D., Rahman, K.S., Bower, B.D., Dismuke, D.J., Falvo, M.R., Griffith, J.D., Harvey, S.C., and Asokan, A. (2013). Biophysical and ultrastructural characterization of adeno-associated virus capsid uncoating and genome release. J. Virol. *87*, 2994–3002.
13. Pasquale, G.D., and Chiorini, J.A. (2006). AAV transcytosis through barrier epithelia and endothelium. Mol. Ther. *13*, 506–516.
14. Watanabe, S., Kanatsu-Shinohara, M., Ogonuki, N., Matoba, S., Ogura, A., and Shinohara, T. (2018). In vivo genetic manipulation of spermatogonial stem cells and their microenvironment by adeno-associated viruses. Stem Cell Rep. *10*, 1551–1564.
15. Bell, C.L., Vandenberghe, L.H., Bell, P., Limberis, M.P., Gao, G.-P., van Vilet, K., Agbandje-McKenna, M., and Wilson, J.M. (2011). The AAV9 receptor and its modification to improve in vivo lung gene transfer in mice. J. Clin. Invest. *121*, 2427–2435.
16. Kohrogi, T., Yokoyama, M., Taguchi, T., Kitamura, Y., and Tutikawa, K. (1983). Effect of the Slt mutant allele on the production of tissue mast cells in mice. J. Hered. *74*, 375–377.
17. Rubin, B.P., Singer, S., Tsao, C., Duensing, A., Lux, M.L., Ruiz, R., Hibbard, M.K., Chen, C.J., Xiao, S.,, Tuveson, D.A., et al. (2001). KIT activation is a ubiquitous feature of gastrointestinal stromal tumors. Cancer Res. *61*, 8118–8121.
18. Dalkara, D., Byrne, L.C., Klimczak, R.R., Visel, M., Yin, L., Merigan, W.H., Flannery, J.G., and Schaffer, D.V. (2013). In vivo-directed evolution of a new adeno-associated virus for therapeutic outer retinal gene delivery from the vitreous. Sci. Transl. Med. *5*, 189ra76.
19. Obata, Y., and Kono, T. (2002). Maternal primary imprinting is established at a specific time for each gene throughout oocyte growth. J. Biol. Chem. *277*, 5285–5289.
20. Wang, D., Tai, P.W.L., and Gao, G. (2019). Adeno-associated virus vector as a platform for gene therapy delivery. Nat. Rev. Drug Discov. *18*, 358–378.
21. Shinohara, T., and Kanatsu-Shinohara, M. (2020). Transgenesis and genome editing of mouse spermatogonial stem cells by lentivirus pseudotyped with Sendai virus F protein. Stem Cell Rep. *14*, 447–461.
22. Dixon, R.E., Hwang, S.J., Hennig, G.W., Ramsey, K.H., Schripsema, J.H., Sanders, K.M., and Ward, S.M. (2009). Chlamydia infection causes loss of pacemaker cells and inhibits oocyte transport in the mouse oviduct. Biol. Reprod. *80*, 665–673.
23. Fisher, K.J., Jooss, K., Alston, J., Yang, Y., Haecker, S.E., High, K., Pathak, R., Raper, S.E., and Wilson, J.M. (1997). Recombinant adeno-associated virus for muscle directed gene therapy. Nat. Med. *3*, 306–312.
24. Snyder, R.O., Spratt, S.K., Lagarde, C., Bohl, D., Kaspar, B., Sloan, B., Cohen, L.K., and Danos, O. (1997). Efficient and stable adeno-associated virus-mediated transduction in the skeletal muscle of adult immunocompetent mice. Hum. Gene Ther. *8*, 1891–1900.
25. Eppig, J.J., and O'Brien, M.J. (1996). Development in vitro of mouse oocytes from primordial follicles. Biol. Reprod. *54*, 197–207.
26. Atabiekov, I., Hobeika, E., Sheikh, U., Andaloussi, A.,E., and Al-Hendy, A. (2018). The role of gene therapy in premature ovarian insufficiency management. Biomedicines *6*, 102.
27. Yatsenko, S.A., and Rajkovic, A. (2019). Genetics of human female infertility. Biol. Reprod. *101*, 549–566.
28. Srinivas, S., Watanabe, T., Lin, C.S., William, C.M., Tanabe, Y., Jessell, T.M., and Costantini, F. (2001). Cre reporter strains produced by targeted insertion of EYFP and ECFP into the ROSA26 locus. BMC. Dev. Biol. *1*, 4.
29. Watanabe, S., Kanatsu-Shinohara, M., Ogonuki, N., Matoba, S., Ogura, A., and Shinohara, T. (2017). Adeno-associated virus-mediated delivery of genes to mouse spermatogonial stem cells. Biol. Reprod. *96*, 221–231.
30. Lee, J., Kanatsu-Shinohara, M., Morimoto, H., Kazuki, Y., Takashima, S., Oshimura, M., Toyokuni, S., and Shinohara, T. (2009). Genetic reconstruction of mouse spermatogonial stem cell self-renewal in vitro by Ras-cyclin D2 activation. Cell Stem Cell *5*, 76–86.
31. Lee, J., Matsuzawa, A., Shiura, H., Sutani, A., and Ishino, F. (2018). Preferable in vitro condition for maintaining faithful DNA methylation imprinting in mouse embryonic stem cells. Genes Cells *23*, 146–160.

STAR★METHODS

KEY RESOURCES TABLE

REAGENT or RESOURCE	SOURCE	IDENTIFIER
Antibodies		
Goat anti-human MIS (AMH)	Santa Cruz Biotechnology	Cat#sc-6886; RRID: AB_649207 Lot G2414
Rabbit anti-mouse HSD3B	Trans Genic Inc.	Cat# KO607; RRID: AB_2622227 Lot TG051018
Rat anti-mouse CD4	Invitrogen	Cat# 12-0041-82; RRID: AB_469772 Lot 2063347
Rat anti-mouse CD8	Abcam	Cat# ab22378; RRID: AB_447033 Lot GR296213-1
Rabbit anti-mouse MKI67	Novus Biologicals	Cat# NB110-89719;RRID: AB_1217078; Lot B-1
Rat anti-GFP antibody	Nacalai tesque	Cat#04404-26; Lot M8E4658
Alexa Fluor 647-conjugated goat anti-rabbit IgG	Invitrogen	Cat# A21245; RRID: AB_141775 Lot 2184318
Alexa Fluor 647-conjugated donkey anti-goat IgG	Invitrogen	Cat# A21447 RRID: AB_141844; Lot 1235825
Alexa Fluor 568-conjugated goat anti-rat IgG	Invitrogen	Cat# A11077; RRID: AB_141874 Lot 1692966
Alexa Fluor 488-conjugated goat anti-rabbit IgG	Invitrogen	Cat# A11008 RRID: AB_143165; Lot 2179202
Alexa Fluor 555-conjugated donkey anti-goat IgG	Invitrogen	Cat# A21432 RRID: AB_141788; Lot 2155590
Alexa Fluor 647-conjugated donkey anti-rabbit IgG	Invitrogen	Cat# A31573; RRID: AB_2536183; Lot 2083195
Alexa Fluor 488-conjugated donkey anti-rat IgG	Invitrogen	Cat# A21208; RRID: AB_141709; Lot 2180272
Mouse anti-beta-actin antibody	SIGMA	Cat# A5441; RRID: AB_476744; Source 22190126; Batch 0000088083
Mouse anti-KITL antibody	Santa Cruz Biotechnology	Cat# sc-13126; RRID: AB_628238; Lot K2817
Mouse anti-MCHERRY antibody	Takara	Cat# 632543; RRID: AB_2307319; Lot 1706595A
HRP (horseradish peroxidase)-conjugated horse anti-mouse IgG	Cell Signaling	Cat# 7076; RRID: AB_330924; Lot 31
HRP-conjugated horse anti-rabbit IgG	Cell Signaling	Cat #7074; RRID: AB_2099233; Lot 29
In Situ Cell Death Detection Kit, TMR red	Roche	Cat# 12156792910; Lot 49483800
Estradiol Parameter Assay Kit	R&D Systems	Cat# KGE014; RRID: AB_2861157; Lot P263164 & P296234
Mouse FSH (follicle-stimulating hormone) ELISA Kit	MyBioSource	Cat# MBS2507988; Lot F2SUQBQMLF & T9BP5H76D5
Luteinizing Hormone (LH) ELISA Kit	MyBioSource	Cat# MBS2018848; Lot L200930578 & L210903620
Bacterial and virus strains		
pAAV-CAG	Watanabe et al., 2018	Penn Vector Core
pCSII-EF1-MCS	RIKEN	Cat# RDB04378 https://dnaconda.riken.jp/search/RDB_clone/RDB04/RDB04378.html
pAxCcw	RIKEN	Cat# DB00917 https://dnaconda.riken.jp/search/RDB_clone/RDB00/RDB00917.html
pHelper	Agilent Technologies	https://www.chem-agilent.com/contents.php?id=300079

(*Continued on next page*)

Continued

REAGENT or RESOURCE	SOURCE	IDENTIFIER
pAAV-RC	Agilent Technologies	https://www.chem-agilent.com/contents.php?id=300079
pAAV1	Watanabe et al., 2018	Penn Vector Core
pAAV6.2	Watanabe et al., 2018	Penn Vector Core
pAAV9	Watanabe et al., 2018	Penn Vector Core
pAAV-DJ	Cell biolabs	Cat# VPK-420-DJ
pAAV-DJ8	Cell biolabs	Cat# VPK-420-DJ-8
pAAV-7M8	Addgene	Addgene plasmid: 64839
Chemicals, peptides, and recombinant proteins		
Neuraminidase	Sigma	Cat# 11585886001
Experimental models: Organisms/strains		
Mouse: B6.Cg-Kitl < Sl-t>/Rbrc	Kohrogi et al., 1983	RBRC00145 https://knowledge.brc.riken.jp/resource/animal/card?__lang__=ja&brc_no=RBRC00145
Mouse: B6.129X1-*Gt(ROSA) 26Sor*$^{tm1(EYFP)Cos}$/J	Srinivas et al., 2001	JAX:006148
Mouse: B6D2F1/Slc	Japan SLC, Shizuoka, Japan	http://www.jslc.co.jp/animals/mouse.php
Oligonucleotides		
Primers used for PCR	This paper	Table S1
Recombinant DNA		
pAAV-CAG-*mCherry*	Watanabe et al., 2018	mCherry cDNA: Dr. Michiyuki Matsuda, Kyoto University
pAAV-CAG-*Kitl*	Watanabe et al., 2018	Kitl cDNA: Dr. Shin-ichi Hayashi, Tottori University
pAAV-CAG-mNG	This paper	mNG cDNA: purchased from Nacalai tesque https://www.nacalai.co.jp/Fount/allele_mneongreen.html
AxCAN-*Egfp*	Takehashi et al., 2007	EGFP cDNA: Dr. Saito Izumu, University of Tokyo
CSII-EF1-IRES-Venus	RIKEN	Cat# RDB04384 https://dnaconda.riken.jp/search/RDB_clone/RDB04/RDB04384.html
Software and algorithms		
cellSens V2.3	Olympus	https://www.olympus-lifescience.com/en/software/cellsens/
Fluoview FV31S-SW	Olympus	https://www.olympus-lifescience.com/en/search-results/?0%5BCMS%3A%3AMeta%5D%5Bsearch%5D=FV31
ImageJ1.53k	National Institute of Health	https://imagej.nih.gov/ij/index.html

RESOURCE AVAILABILITY

Lead contact

Further information and requests for resources and reagents should be directed to and will be fulfilled by the Lead Contact, Takashi Shinohara (tshinoha@virus.kyoto-u.ac.jp).

Materials availability

All unique/stable reagents generated in this study are available from the lead contact with a completed Materials Transfer Agreement.

Data and code availability

All data reported in this paper will be shared by the lead contact upon request. This paper does not report the original code. Any additional information required to reanalyze the data in this paper is available from the lead contact upon request.

EXPERIMENTAL MODEL AND SUBJECT DETAIL

All experiments utilizing animals were approved by The Institutional Animal Care and Use Committee of Kyoto University. All animals were maintained under conditions of *ad libitum* water and food with constant light-dark cycles. For *in vivo* screening and tracer

experiments, we used 4- to 5-week-old C57BL/6 (B6) mice. In some experiments, we used 4- to 8-week-old *R26R-Eyfp* mice (a gift from Dr. F. Costantini, Columbia University Medical Center, NY).[28] For fertility restoration experiments, 4- to 8-week old B6.Cg-Kitl < Sl-t>/Rbrc mice with a mixed B6, DBA/2 background were used (RIKEN BRC, Ibaraki, Japan).[16]

METHOD DETAILS

Virus production

AAV production was performed as previously described.[29] In brief, an AAV vector plasmid (pAAV-CAG-*mCherry*, pAAV-CAG-*Kitl* or pAAV-CAG-*Cre*), an adenovirus helper plasmid (pHelper; Agilent Technologies, Santa Clara, CA), and an AAV helper plasmid (pAAV-RC; Agilent Technologies, pAAV1, pAAV6.2, pAAV9; gift from Penn Vector Core [University of Pennsylvania, PA], pAAV-DJ, pAAV-DJ8; Cell biolabs, San Diego, CA, and pAAV-7M8; Addgene, Boston, MA) were transiently transfected into 293T cells. Viral titers (in vector genomes (VG)/mL) were determined by real-time PCR using FastStart Universal SYBR Green Master Mix (Roche Diagnostic GmbH, Penzberg, Germany) and specific primers, as described previously (Watanabe et al., 2018). For screening, the titer of the virus was 1×10^{12} vector genomes/mL. In some experiments, we also used AxCAN-*Egfp* (RIKEN BRC), CSII-EF1-IRES-*Venus* (RIKEN BRC) and CSII-EF1-*Kitl*. The titer of AxCAN-*Egfp* was 2.0×10^{8} plaque-forming units/mL. The titers of CSII-EF1-IRES-*Venus* and CSII-EF1-*Kitl* were 1.5×10^{9} transducing units (TU)/mL and 2.8×10^{9} TU/mL, respectively.

Microinjection into ovaries

For the ovarian injections, two ventral-lateral flank incisions were made approximately 2-mm caudal to the last rib. The ovary was pulled out by fine forceps. Care was taken not to injure blood vessels and the ovarian tunica. By gently holding a fat pad around the oviduct and ovarian bursa, a pipette was advanced with the micromanipulator, and a glass needle was inserted under the tunica albuginea of the ovary. Filling was confirmed by adding a small amount of trypan blue. Approximately 2-μL of FITC-dextran (50 mg/mL; Sigma, St. Louis, MO) or virus particles was microinjected into the ovarian stroma. For dextran injections, the ovaries were recovered 30-min after injection. In some experiments, neuraminidase (Sigma) was added to enhance transfection efficiency, as described previously.[14] Males were added at least 2 weeks after microinjection.

Measurement of hormones

The levels of estrogen, LH, and FSH in the serum of mice were measured by a competitive-based enzyme-linked immunosorbent assay (ELISA) using an estrogen ELISA kit (R & D systems, Minneapolis, MN), an LH ELISA Kit, and a mouse FSH ELISA kit (both from MyBiosource, San Diego, CA). Absorbance at a wavelength of 450-nm was measured using an automated microplate reader. Data were expressed as pg of estrogen per mL of serum, and ng of LH and FSH per mL of serum.

Analysis of ovaries

Animals were sacrificed at indicated time points after microinjection, and ovaries were fixed in 4% paraformaldehyde for 2-h, followed by embedding in paraffin or Tissue-Tek OCT compound. For analysis of follicle development, histological sections were stained with hematoxylin and eosin for counting. For analysis of *R26R-Eyfp* mice, ovaries were examined under the UV light. Immunostaining of cryosections was performed, as described previously.[29] The total area of MCHERRY expression was measured using a cellSens V2.3 (Olympus, Tokyo, Japan).

Immunohistochemistry

For immunohistochemistry experiments, testis samples were fixed in 4% paraformaldehyde for 2-h, and then embedded in Tissue-Tek OCT compound for cryosectioning. Immunostaining of cryosections was carried out by treating the samples with 0.1% Triton-X in phosphate-buffered saline (PBS). After immersion in blocking buffer (0.1%Tween 20, 1% bovine serum albumin and 1% donkey or goat serum in PBS) for > 1-h, samples were incubated with the indicated primary antibodies at 4°C overnight. After three washes with 0.1%Tween 20 in PBS, samples were incubated with the secondary antibody.

RT-PCR

For total RNA extraction, samples were dissolved in TRIzol (Invitrogen). First- strand cDNA was produced using a Verso cDNA Synthesis Kit (Thermo Fisher Scientific, Waltham, MA). Transcript levels were normalized to those of *Hprt*. The PCR conditions were as follows: 95 °C for 10-min, followed by 40 cycles at 95°C for 15-s and 60°C for 1-min. Each PCR was performed in least triplicate.

DNA analysis

Genomic DNA was isolated from the offspring using a standard phenol/chloroform extraction procedure and ethanol precipitation. PCR was performed using specific primers (Table S1). To detect viral DNA by Southern blotting, we digested 20 μg of DNA with indicated restriction enzymes, and separated the fragments by electrophoresis on a 1.0% agarose gel. DNA was transferred and blotted onto a nylon membrane (Hybond-N+;Amersham Biosciences, Buckinghamshire, UK). Hybridization was performed according to a standard protocol using the entire AAV virus as a probe. The membrane was hybridized for 16-h at 65°C with a ^{32}P-labeled probe.

COBRA

Genomic DNA was treated with sodium bisulfite, which deaminates unmethylated cytosines to uracils but does not affect 5-methylated cytosines. The DNA was used as a template to amplify differentially methylated regions using specific primers.[30] The PCR product was digested with the indicated restriction enzymes, which recognize DNA sequences containing CpG in the original unconverted DNA.

Bisulfite sequencing

DNA methylation analysis was performed as described previously.[31] Bisulphite-treated DNA was amplified by PCR using specific primer sets, and the amplified PCR products were purified using AMPure XP (Beckman Coulter) according to the manufacturer's protocols. Subsequently, the purified PCR products were amplified by nested PCR primers conjugated with Ion PGM Barcode X (comprising 13 bases each) and barcode adapter GAT, then sequenced. Sequence data were processed as FASTA format files, and DNA methylation analyses were performed using the QUMA: Quantification tool for methylation analysis.

QUANTIFICATION AND STATISTICAL ANALYSIS

Significant differences between means for single comparisons were determined by Student's t-tests. All data were analyzed by Microsoft Excel. All the results are expressed as mean ± SEM. A value of $p < 0.05$ was considered to be statistically significant.